

See discussions, stats, and author profiles for this publication at: <https://www.researchgate.net/publication/276421344>

Diamond Crystallization from an Antimony–Carbon System under High Pressure and Temperature

ARTICLE *in* CRYSTAL GROWTH & DESIGN · MAY 2015

Impact Factor: 4.89 · DOI: 10.1021/acs.cgd.5b00310

CITATIONS

3

READS

29

6 AUTHORS, INCLUDING:



Alex G. Sokol

Russian Academy of Sciences

75 PUBLICATIONS 1,330 CITATIONS

SEE PROFILE

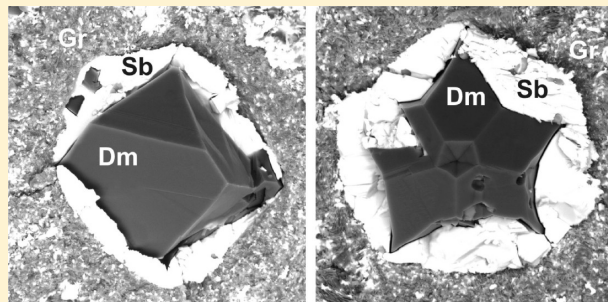
Diamond Crystallization from an Antimony–Carbon System under High Pressure and Temperature

Yuri N. Palyanov,* Yuri M. Borzdov, Igor N. Kupriyanov, Yuliya V. Bataleva, Alexander F. Khokhryakov, and Alexander G. Sokol

Sobolev Institute of Geology and Mineralogy, Siberian Branch of Russian Academy of Sciences, Koptyug ave 3, Novosibirsk, 630090, Russia

Novosibirsk State University, Novosibirsk, 630090, Russia

ABSTRACT: We report the results of an experimental study on diamond crystallization in the Sb–C system under HPHT conditions. The experiments were run at pressures of 6.3 and 7.5 GPa in the temperature range of 1500–1800 °C for 1 to 40 h. Diamond crystallization via spontaneous nucleation and growth on the seed crystals has been established. It is shown that the kinetic factor plays a crucial role in diamond crystallization in the Sb–C system. For run duration of 40 h the minimal P – T parameters of diamond growth on the seed crystals are found to be 6.3 GPa and 1500 °C, while the minimal parameters for spontaneous nucleation are 7.5 GPa and 1600 °C.



INTRODUCTION

In the 1950s, the first successful diamond-synthesis experiments, which have laid the foundations for industrial production of diamond, were performed in metal–carbon systems.^{1,2} At pressures of 5–6 GPa and temperatures in the range of 1350–1600 °C, melts of transition metals (Fe, Ni, Co, Mn, etc.) and their alloys provide conversion of graphite to diamond in experiments lasting for a few minutes. Taking into account the relatively high solubility of carbon in melts of these metals and the extremely high rates of the graphite-to-diamond transformation, these melts were classified as the solvent–catalysts. This approach used for other solvents of carbon in the above-mentioned range of P – T parameters did not result in synthesis of diamond and many compounds, including carbonates, chlorides, sulfides, oxides, and silicates, were referred to as graphite-producing solvents of carbon.³ In the early 1990s, it has been demonstrated that applying significantly higher pressures (7–7.7 GPa) and temperatures (2000–2150 °C) diamond could be synthesized in melts of carbonates,⁴ sulfates and hydroxides,⁵ phosphorus,⁶ and in the H₂O–C system.⁷ Further experimental studies revealed the kinetic nature of diamond nucleation and growth for many nonmetallic solvents and showed that the P – T parameters of diamond crystallization can be significantly reduced. It has been demonstrated that the onset of diamond crystallization can be preceded by a long induction period over which diamond nucleation does not take place and whose duration increases almost exponentially with decreasing temperature.^{8–11} The experimental data on diamond synthesis in phosphorus–carbon^{6,12} and sulfur–carbon^{13,14} systems with different experimental duration up to several tens of hours can be taken as the most illustrative examples. These findings clearly

indicate that kinetic effects play a crucial role in diamond nucleation and growth in nonmetallic media. This fact makes it possible to substantiate new attempts at diamond synthesis using different carbon solvents that were unsuccessful in earlier experiments. Such studies are of particular interest providing both new information on the mechanisms of diamond nucleation and growth and the potential possibility of synthesizing diamonds with unique properties.

Among the substances whose ability to catalyze diamond synthesis deserves a detailed examination, of particular interest is antimony. Sb is a group V element and if incorporated in diamond as an atomic impurity may potentially produce a donor state. In silicon, Sb forms a shallow donor level lying 0.039 eV below the conduction band minimum.¹⁵ Recent theoretical works indeed predicted that the donor levels of pnictogen impurities (N, P, As, and Sb) in diamond become increasingly shallow with increasing atomic number.^{16,17} This trend, however, was accompanied by a concomitant increase in the formation energy, and hence a decrease in bulk solubility. On the other hand, despite the fact that theory also predicts that phosphorus is insoluble in bulk diamond,^{18,19} doping of diamond with P has been successfully realized by both chemical vapor deposition²⁰ (CVD) and high-pressure high-temperature (HPHT) synthesis in the P–C system.²¹ Incorporation of phosphorus impurities in concentrations greatly exceeding the solubility level suggests the dominating role of the growth kinetics and surface processes, and provides a potential route for doping diamond with relatively large impurity atoms. Previous attempts at HPHT synthesis of diamond with

Received: March 5, 2015

antimony as the solvent–catalyst were unsuccessful. Strong²² found that Sb did not catalyze the formation of diamond at 6 GPa and temperatures up to 1400 °C. More recently, Lv et al.²³ reported that diamond could not be synthesized in the Sb–C systems at considerably higher pressure of 9.6 GPa and temperature of 1850 °C. However, in both these works the experiments were performed with rather short run times, 10 and 30 min in refs 22 and 23, respectively. Given the established kinetic effects in diamond synthesis with non-metallic solvent–catalysts, it is therefore challenging to re-examine the catalytic ability of antimony over a broad range of experimental durations.

EXPERIMENTAL SECTION

Experiments in the Sb–C system were performed using a multi-anvil split-sphere apparatus²⁴ at pressures of 6.3 and 7.5 GPa in a 1500–

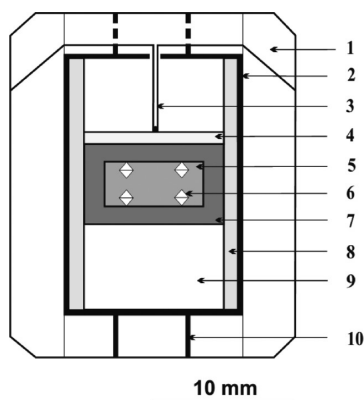


Figure 1. High pressure cell used for diamond crystallization in the Sb–C system. 1 - container (ZrO₂); 2 - cylindrical graphite heater; 3 - PtRh6/PtRh30 thermocouple; 4 - MgO disc; 5 - Sb; 6 - diamond seed; 7 - graphite container; 8 - MgO sleeve; 9 - ZrO₂ cylinder; 10 - Mo input leads.

1800 °C temperature range. The experimental duration was varied from 1 to 40 h. The high-pressure cells had the shape of a trigonal prism with sizes $19 \times 19 \times 22 \text{ mm}^3$ and $21.1 \times 21.1 \times 25.4 \text{ mm}^3$ for experiments at 7.5 and 6.3 GPa, respectively. Temperature was measured in each experiment using a PtRh30/PtRh6 thermocouple, whose junction was placed near the crystallization capsule. Details of the calibration of the P – T parameters have been presented elsewhere.^{25,26} The starting materials were a graphite rod (99.99%

purity), antimony with purity not less than 99.99%, and synthetic diamonds as the seed crystals. The latter were either small (ca. 0.5 mm) cuboctahedral crystals or larger (ca. 2 mm) {111} plates cut from diamond crystals. Graphite rods were machined into thick-walled (1–1.5 mm) capsules with the inner diameter of 7 mm for the experiments at 6.3 GPa and 5 mm for the experiments at 7.5 GPa. Pressed Sb cylinders with diamond seed crystals were placed inside the graphite capsules as shown in Figure 1. After experiments, the produced diamond crystals were studied using an Axio Imager.Z2m optical microscope and a LEO 420 scanning electron microscope. The metal composition was controlled using an energy dispersive spectrometer attached to the scanning electron microscope. Formation of small diamond crystals was confirmed by Raman spectroscopy. Raman and photoluminescence (PL) spectra were measured using a Horiba J.Y. LabRAM HR spectrometer and a 523 nm solid state laser as an excitation source. A Linkam FTIR600 heating/freezing stage was used for PL measurements at about 80 K.

RESULTS AND DISCUSSION

The results of experiments in the Sb–C system at 6.3 and 7.5 GPa and temperatures ranging from 1500 to 1800 °C are summarized in Table 1. Complete melting of antimony was clearly detected in the entire range of P – T parameters under study. At 6.4 GPa no diamond nucleation was established at temperatures of 1500 and 1600 °C despite the fact that experimental duration ranged from 10 to 40 h.

At 7.5 GPa and 1600 °C neither spontaneous nucleation of diamond nor diamond growth on the seed crystals was detected in a 5 h experiment. A significant increase in experimental duration to 40 h resulted in diamond growth on the seed crystals and spontaneous crystallization of diamond along the entire interface between the graphite capsule and the antimony melt. Although the degree of the graphite-to-diamond transformation was negligible and estimated as <1%, this experiment is worthy of note illustrating the initial stage of diamond nucleation. Figure 2a shows a fragment of a graphite disc with diamond crystals. With significant magnification one can see that diamonds at the graphite–melt interface are represented by individual octahedral crystals (Figure 2b), contact twinned octahedra (Figure 2c,d), cyclic twins shaped as five-pointed stars (Figure 2e), or irregularly shaped aggregates (Figure 2f).

Crystal size varies from 5 to 50 μm . In all cases, diamond crystals, twins, and aggregates are surrounded by an antimony layer with thickness varying from several micrometers to 15 μm , which separates diamond from graphite. This fact unambiguously indicates that diamond crystallization took

Table 1. Experimental Results^a

run N	P , GPa	T , °C	time, h	diamond growth on seeds	diamond nucleation	α (%) Gr→Dm transformation
SB-1257	6.3	1500	20	-	-	0
SB-1259	6.3	1500	40	+	-	0
SB-1253	6.3	1600	10	-	-	0
SB-1261	6.3	1600	40	+	-	0
SB-1239	7.5	1600	5	-	-	0
SB-1243	7.5	1600	40	+	+	<1
SB-1233	7.5	1700	1	-	-	0
SB-1236	7.5	1700	30	+	+	10
SB-1244	7.5	1700	40	+	+	80
SB-1161	7.5	1800	1	-	-	0
SB-1168	7.5	1800	10	+	+	3–5
SB-1169	7.5	1800	19	*	+	50

^a“+”, was observed; “-”, was not observed; *, run without seed crystals. α is the degree of the graphite-to-diamond transformation, $\alpha = M_{\text{Dm}}/(M_{\text{Dm}} + M_{\text{Gr}})100$, where M_{Dm} is the mass of obtained diamond and M_{Gr} is the mass of residual graphite. Dm - diamond, Gr - graphite.

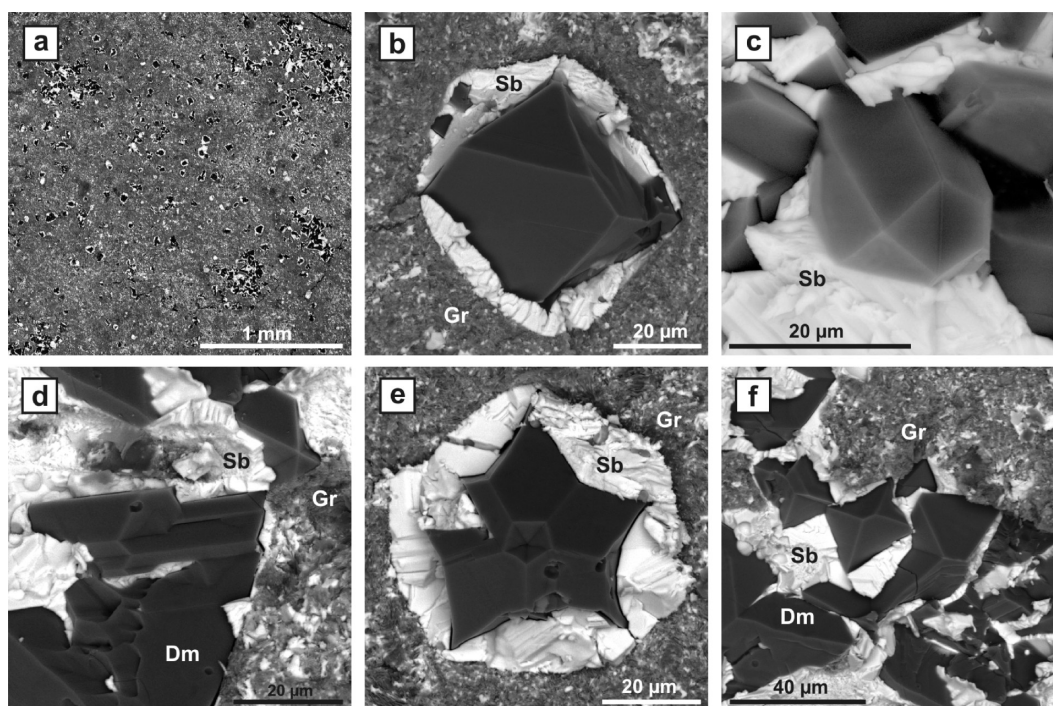


Figure 2. SEM micrographs of diamond crystals synthesized in the antimony–carbon system: (a) a fragment of the graphite disk with diamond crystals at the interface with Sb melt, (b) octahedral diamond crystals in Sb melt at the graphite–melt interface, (c,d) contact twins of octahedral crystals in Sb melt, (e) a five-pointed star cyclic twin of diamond octahedrons surrounded by quenched Sb melt, (f) crystals, twins, and overgrowths of diamond.

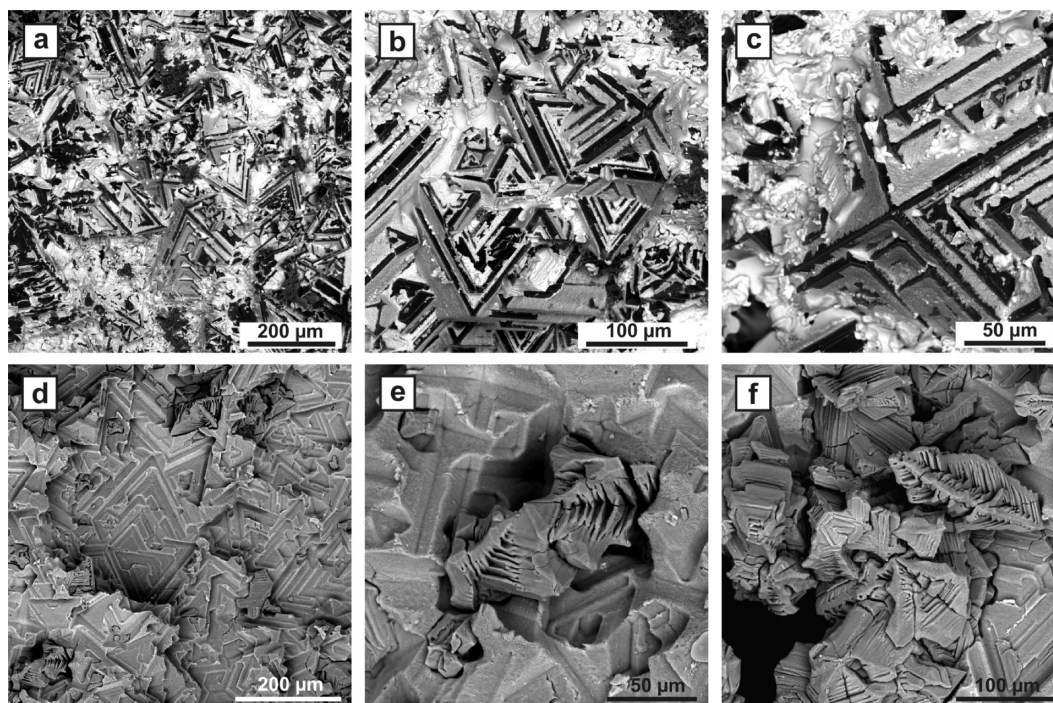


Figure 3. SEM micrographs of diamond crystals synthesized in the antimony–carbon system: (a,b,c) octahedrons coated with a thin film of quenched Sb melt, (d) imprints of a polycrystalline aggregate of octahedral diamonds on the graphite capsule, after dissolution of Sb, (e,f) skeletal diamond crystals and aggregates after dissolution of Sb.

place via the FG (Film Growth) mechanism which is typical of all diamond-forming metal–carbon systems.²⁷ The uniform distribution of diamond crystallization centers over the entire inner surface of the graphite capsule with density of $\sim 10^2 \text{ mm}^{-2}$ provides additional evidence for a negligible temperature

gradient in the crystallization capsule. Diamond crystallization was considerably activated by increasing temperature to 1700 °C at 7.5 GPa. The effect of the experimental duration factor is evident at these conditions. Thus, neither diamond growth nor nucleation was observed in a 1 h experiment, whereas in

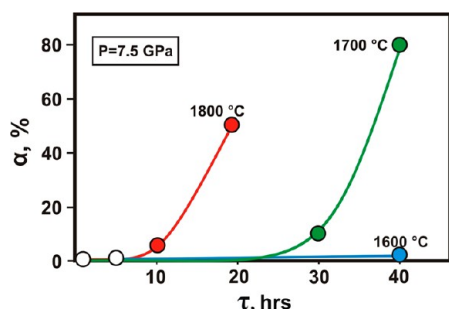


Figure 4. Degree of the graphite-to-diamond transformation (α) versus run duration (τ) for experiments at 7.5 GPa and 1600–1800 °C.

experiments with duration of 30 and 40 h the degree of graphite-to-diamond transformation was ~10% and ~80%, respectively. Diamond nucleates at the graphite–metal interface boundary and grows due to carbon diffusion through the antimony melt film. The crystallization front of diamond propagates from the inner wall of the graphite capsule toward the outer one. The polycrystalline aggregate consisting of relatively large octahedral diamond crystals (~100 μm) with step-like faces coated with a thin layer of quenched antimony melt is eventually formed (Figure 3a–c). After antimony is dissolved in nitric acid, the indentations of the polycrystalline aggregate of octahedral diamonds are clearly seen on the graphite capsule (Figure 3d). Diamonds are represented by typical skeletal crystals and their aggregates (Figure 3e,f). Temperature increasing to 1800 °C significantly accelerates the reaction between antimony and graphite but does not change the general pattern of diamond crystallization and its kinetic dependence. No diamond formation was detected in the 1 h

experiment performed at 7.5 GPa and 1800 °C. These parameters are close to those used by Lv et al.²³ for the Sb–C system, so that the absence of diamond nucleation as established in the present study is in fair agreement with the previous work.²³ With increasing experimental duration to 10 and 19 h the degree of the graphite-to-diamond transformation increases to 3–5% and ~50%, respectively. Figure 4 shows the dependence of the degree of the graphite-to-diamond transformation (α) on the experimental duration in the temperature range of 1600–1800 °C at 7.5 GPa. The obtained data clearly demonstrate the effect of kinetics on diamond nucleation and explain why previous attempts at diamond synthesis in the Sb–C system were unsuccessful. As also follows from Figure 4 temperature is another important factor controlling diamond synthesis in this system.

Diamond growth on the seed crystals is also found to require experiments of significant duration (see Table 1). Several examples illustrating the variations of the growth relief on diamond seed crystals are demonstrated in Figure 5. At 7.5 GPa and 1600 °C vicinal structures of triangular or hexagonal shape are formed on the {111} cleavage plane (Figure 5a,b,c). At 1700 °C clear manifestations of island growth were detected on octahedral faces (Figure 5d). At a pressure of 6.3 GPa no diamond growth on the seed crystals was detected after 10 h at 1600 °C, and 20 h at 1500 °C. However, in 40 h runs at these temperatures marked growth on the seed crystals was observed for both {111} (Figure 5e) and {100} (Figure 5f) faces, exhibiting triangular-shaped vicinal structures and specific growth elements, respectively. In all the experiments where diamond growth on seed crystals was observed, the grown layer thickness was less than 10 μm . These results indicate that both diamond synthesis via the FG mechanism and diamond growth

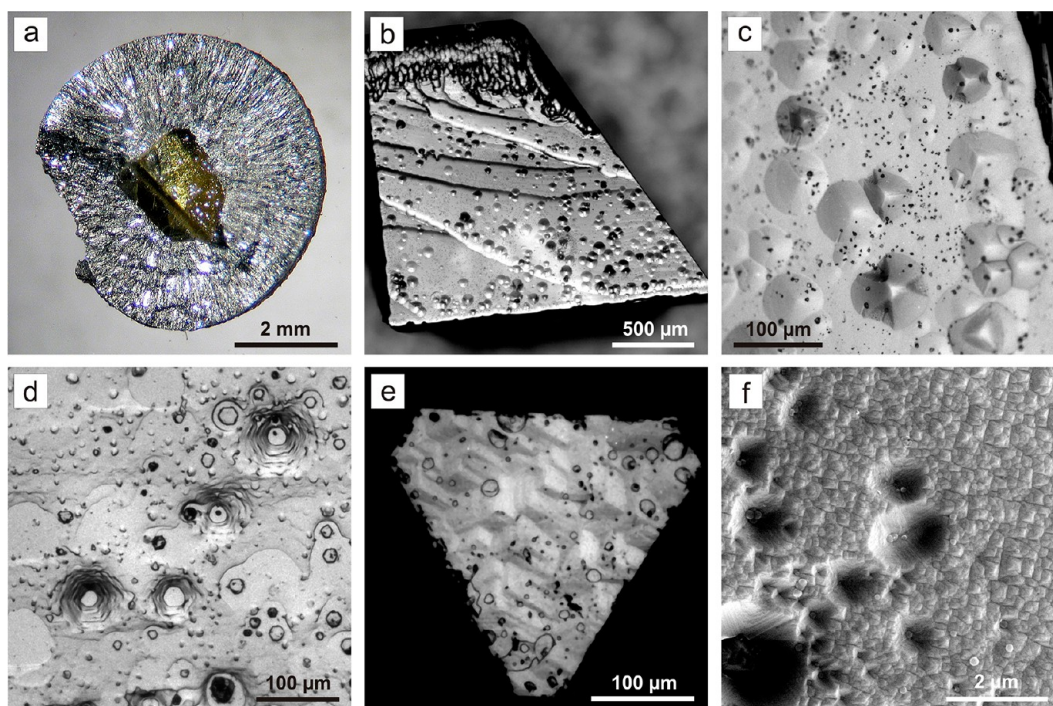


Figure 5. Growth microrelief of diamond seed crystals in the Sb–C system: (a) overall view of a diamond seed crystals in Sb matrix and (b,c) growth vicinals on the {111} faces after an experiment at 7.5 GPa and 1600 °C; (d) formation of island growth patterns on the {111} faces at 7.5 GPa and 1700 °C; (e) trigonal vicinals on the {111} faces and (f) microrelief on the {100} faces at 6.3 GPa and 1600 °C. (a–e) optical micrographs, (f) SEM micrograph.

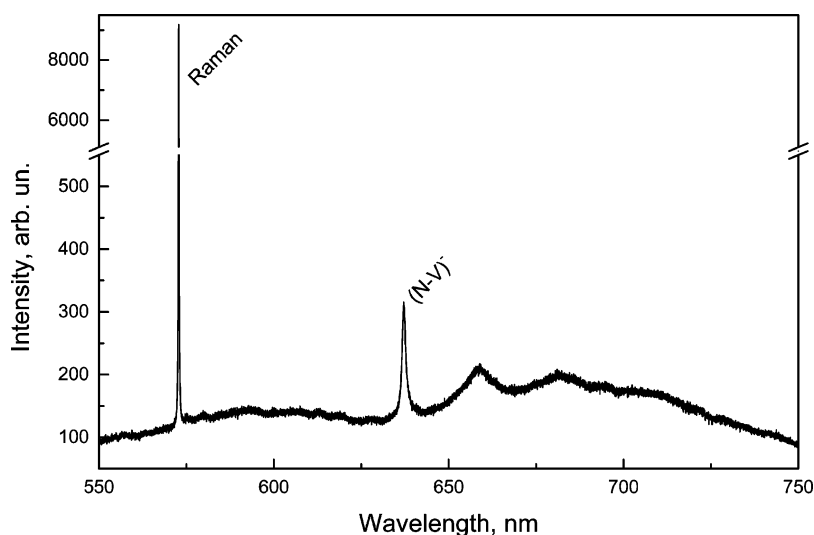


Figure 6. Typical PL/Raman spectrum of diamond synthesized in the Sb–C system (run SB-1244).

on seed crystals via the TGG (temperature gradient growth) mechanism can take place in antimony melt.

Due to relatively small sizes of the synthesized diamond crystals it was not possible to study them using infrared absorption spectroscopy. We however note that the crystals look colorless suggesting low concentrations of impurities. In fact, for diamond containing shallow donors or acceptors one would expect bluish coloration as observed for phosphorus- or boron-doped diamond. Raman/PL measurements performed for a number of crystals synthesized in runs SB-1169 and SB-1244 yielded similar spectra, and a representative one is shown in Figure 6. It comprises an intense peak at 572 nm due to the first-order Raman scattering and a weak vibronic system related to the negatively charged nitrogen-vacancy (N–V) centers (zero-phonon line at 637 nm). It is interesting that no PL caused by neutral N–V centers (the 575 nm system) was observed. The occurrence of the negatively charged centers implies that another species acting as electron donor should also occur in the crystals. More detailed investigations of the diamond crystals synthesized in the Sb–C system are currently under way.

SUMMARY

The results of the present study allow us to unequivocally classify antimony as the solvent–catalyst of diamond synthesis and prove that the kinetic factor plays a crucial role in diamond crystallization in the Sb–C system. The revealed regularities indicate that diamond crystallization from carbon solution in antimony melt takes place via both the FG and TGG mechanisms which are typical of metallic²⁷ and nonmetallic²⁸ melts. The minimal P – T parameters of diamond growth on seed crystals in the Sb–C system were 6.3 GPa and 1500 °C, while the minimal nucleation parameters were 7.5 GPa and 1600 °C. The duration of experiments required for diamond growth and nucleation at these P – T parameters was 40 h. Octahedron is the stable form of diamond growth in the studied range of conditions. With the induction period preceding diamond nucleation and growth in the Sb–C system taken into account, which is rather high and depends on P – T parameters, it is reasonable to apply the “kinetic” approach for other promising media where diamond synthesis has not been realized thus far.

AUTHOR INFORMATION

Corresponding Author

*E-mail: palyanov@igm.nsc.ru. Fax: +7-(383)-3307501.

Notes

The authors declare no competing financial interest.

ACKNOWLEDGMENTS

This work was supported by the Russian Science Foundation under Grant No. 14-27-00054.

REFERENCES

- (1) Bundy, F. P.; Hall, H. T.; Strong, H. M.; Wentorf, J. R. *Nature* **1955**, *176*, 51–55.
- (2) Bovenkerk, H. P.; Bundy, F. P.; Hall, H. T.; Strong, H. M.; Wentorf, J. R. *Nature* **1959**, *184*, 1094–1098.
- (3) Wentorf, R. H. In *Advances in High Pressure Research*; Wentorf, R. H., Ed.; Academic Press: London, 1974; Vol. 4, pp 249–281.
- (4) Akaishi, M.; Kanda, H.; Yamaoka, S. *J. Cryst. Growth* **1990**, *104*, 578–581.
- (5) Akaishi, M.; Kanda, H.; Yamaoka, S. *Jpn. J. Appl. Phys.* **1990**, *29*, L1172–L1174.
- (6) Akaishi, M.; Kanda, H.; Yamaoka, S. *Science* **1993**, *259*, 1592–1593.
- (7) Yamaoka, S.; Akaishi, M.; Kanda, H.; Osawa, T. *J. Cryst. Growth* **1992**, *125*, 375–377.
- (8) Pal'yanov, Yu. N.; Sokol, A. G.; Borzdov, Yu. M.; Khokhryakov, A. F.; Sobolev, N. V. *Nature* **1999**, *400*, 417–418.
- (9) Akaishi, M.; Yamaoka, S. *J. Cryst. Growth* **2000**, *209*, 999–1003.
- (10) Sokol, A. G.; Palyanov, Yu. N.; Palyanova, G. A.; Tomilenko, A. A. *Geochem. Int.* **2004**, *42*, 830–838.
- (11) Yamaoka, S.; Kumar, S. M. D.; Kanda, H.; Akaishi, M. *Diamond Relat. Mater.* **2002**, *11*, 118–124.
- (12) Palyanov, Yu. N.; Kupriyanov, I. N.; Sokol, A. G.; Khokhryakov, A. F.; Borzdov, Yu. M. *Cryst. Growth Des.* **2011**, *11*, 2599–2605.
- (13) Sato, K.; Katsura, T. *J. Cryst. Growth* **2001**, *223*, 189–194.
- (14) Palyanov, Yu. N.; Kupriyanov, I. N.; Borzdov, Yu. M.; Sokol, A. G.; Khokhryakov, A. F. *Cryst. Growth Des.* **2009**, *9*, 2922–2926.
- (15) Sze, S. M. *Physics of Semiconductor Devices*, 2nd ed.; Wiley-Interscience: New York, 1981.
- (16) Sque, S. J.; Jones, R.; Goss, J. P.; Briddon, P. R. *Phys. Rev. Lett.* **2004**, *92*, 017402.
- (17) Goss, J. P.; Briddon, P. R.; Sque, S. J.; Jones, R. *Diamond Relat. Mater.* **2004**, *13*, 684–690.
- (18) Kajihara, S. A.; Antonelli, A.; Bernholc, J.; Car, R. *Phys. Rev. Lett.* **1991**, *66*, 2010–2013.

- (19) Goss, J. P.; Jones, R.; Heggie, M. I.; Ewels, C. P.; Briddon, P. R.; Öberg, S. *Phys. Rev. B* **2002**, *65*, 115207.
- (20) Nesladek, M. *Semicond. Sci. Technol.* **2005**, *20*, R19–R27.
- (21) Kanda, H.; Koizumi, S. In *Innovative Superhard Materials and Sustainable Coatings for Advanced Manufacturing*; Lee, J., Novikov, N., Eds.; Springer: Berlin, 2005; pp 233–245.
- (22) Strong, H. M. *J. Chem. Phys.* **1963**, *39*, 2057–2062.
- (23) Lv, S. J.; Hong, S. M.; Yuan, C. S.; Hu, Y. *Appl. Phys. Lett.* **2009**, *95*, 242105.
- (24) Palyanov, Yu. N.; Borzdov, Yu. M.; Khokhryakov, A. F.; Kupriyanov, I. N.; Sokol, A. G. *Cryst. Growth Des.* **2010**, *10*, 3169–3175.
- (25) Pal'yanov, Yu. N.; Sokol, A. G.; Borzdov, Yu. M.; Khokhryakov, A. F. *Lithos* **2002**, *60*, 145–159.
- (26) Sokol, A. G.; Palyanov, Yu. N.; Surovtsev, N. V. *Diamond Relat. Mater.* **2007**, *16*, 431–434.
- (27) Kanda, H.; Fukunaga, O. In *High-Pressure Research in Geophysics*; Akimoto, S., Manghnani, M. H., Eds.; Academic Press: Tokyo, 1982; pp 525–535.
- (28) Palyanov, Yu. N.; Shatsky, V. S.; Sobolev, N. V.; Sokol, A. G. *Proc. Natl. Acad. Sci. U.S.A.* **2007**, *104*, 9122–9127.